Raft Partitioning and Dynamic Behavior of Human Placental Alkaline Phosphatase in Giant Unilamellar Vesicles

Nicoletta Kahya,[‡] Deborah A. Brown,[§] and Petra Schwille*[,‡]

Max Planck Institute of Molecular Cell Biology and Genetics, Dresden University of Technology, Pfotenhauerstrasse 108, 01307 Dresden, Germany, and Department of Biochemistry and Cell Biology, State University of New York, Stony Brook, New York 11794-5215

Received December 8, 2004; Revised Manuscript Received March 25, 2005

ABSTRACT: Much attention has recently been drawn to the hypothesis that cellular membranes organize in functionalized platforms called rafts, enriched in sphingolipids and cholesterol. The notion that glycosylphosphatidylinositol (GPI)-anchored proteins are strongly associated with rafts is based on their insolubility in nonionic detergents. However, detergent-based methodologies for identifying raft association are indirect and potentially prone to artifacts. On the other hand, rafts have proven to be difficult to visualize and investigate in living cells. A number of studies have demonstrated that model membranes provide a valuable tool for elucidating some of the raft properties. Here, we present a model membrane system based on domain-forming giant unilamellar vesicles (GUVs), in which the GPI-anchored protein, human placental alkaline phosphatase (PLAP), has been functionally reconstituted. Raft morphology, protein raft partitioning, and dynamic behavior have been characterized by fluorescence confocal microscopy and fluorescence correlation spectroscopy (FCS). Approximately 20−30% of PLAP associate with sphingomyelin-enriched domains. The affinity of PLAP for the liquid-ordered (l_o) phase is compared to that of a nonraft protein, bacteriorhodopsin. Next, detergent extraction was carried out on PLAP-containing GUVs as a function of temperature, to relate the lipid and protein organization in distinct phases of the GUVs to the composition of detergent resistant membranes (DRMs). Finally, antibody-mediated cross-linking of PLAP induces a shift of its partition coefficient in favor of the l_o phase.

Many functionally diverse proteins are associated with cellular membranes by a GPI[1] anchor, which consists of an evolutionarily conserved C-terminal post-translational lipid modification (*1*−*3*). Despite the extensive structural information available on the GPI moiety, the functional significance of this ubiquitous membrane anchorage, which is conserved from yeast to humans, is less understood. Some GPI-anchored proteins (GPI-APs), e.g., the decay-accelerating factor (DAF) (*4*) and CD58 (*5*), function equally well when a transmembrane segment replaces the GPI moiety. In other cases, protein function and regulation are strongly impaired in the absence of the GPI anchor, as for the regulation of folate uptake by the GPI-anchored folate receptor (*6*). Especially in mammalian cells, the GPI moiety is thought to be more than just a membrane anchor and has been implicated in a variety of transmembrane and intracellular signaling (*7*, *8*), apical sorting (*9*−*11*), and cell−cell interaction (*12*, *13*) events. It has been suggested that apical sorting and transmembrane signaling occur by association of the GPI anchor with putative cholesterol- and sphingolipid-enriched sorting platforms called "rafts" (*14*−*16*). Furthermore, in the context of their membrane trafficking pathways, GPI-APs are found to be retained in the recycling endocytic compartments (RECs) longer than in other membrane compartments (*17*), and this behavior has been shown to depend on sphingolipid and cholesterol cellular levels (*18*). This triggered the idea that, under some conditions, GPI-APs might associate with lipid rafts.

Commonly conceived, rafts are enriched in sphingolipids and cholesterol, which are thought to intercalate according to a tight and ordered molecular packing (*19*−*21*). The initial observation that cellular membranes were only partially soluble in nonionic detergent, and that the remaining detergent-resistant membranes (DRMs) were enriched in sphingolipids and cholesterol (*11*), has long been used as an operational definition of lipid rafts (*15*, *19*, *20*). Several groups have recovered GPI-APs in DRMs isolated from cell lysates (*11*, *22*−*24*), and these observations have been interpreted as strong evidence of a direct interaction of GPI-APs with raft lipids found in the DRMs (*24*). However, it became evident that, upon detergent treatment, GPI-APs

* To whom correspondence should be addressed. Telephone: +49-351-46340328 or +49-351-46340323. Fax: +49-351-46340342. E-mail: schwille@mpi-cbg.de.

‡ Dresden University of Technology.

§ State University of New York.

[1] Abbreviations: GUVs, giant unilamellar vesicles; LUVs, large unilamellar vesicles; FCS, fluorescence correlation spectroscopy; AFM, atomic force microscopy; GPI, glycosylphosphatidylinositol; PLAP, placental alkaline phosphatase; BRh, bacteriorhodopsin; Rh, rhodamine; DRMs, detergent resistant membranes; l_o, liquid-ordered; l_d, liquid-disordered; DOPC, L-α-dioleoylphosphatidylcholine; SM, *N*-stearoyl-D-erythrosphingosylphosphorylcholine; GM1, porcine brain ganglioside GM1; DiO-C_{18}, 3,3′-dioctadecyloxacarbocyanine perchlorate; DiI-C_{18}, 1,1′-dioctadecyl-3,3,3′,3′-tetramethylindocarbocyanine perchlorate; AF488−CTXB, AlexaFluor488-labeled cholera toxin B subunit; AF633−CTXB, AlexaFluor633-labeled cholera toxin B subunit; CHAPS, 3-[(3-cholamidopropyl)dimethylammonio]-1-propanesulfonic acid; OG, octyl glucoside; ITO, indium tin oxide; DTT, dithiothreitol.

10.1021/bi047429d CCC: $30.25
Published on Web 04/29/2005

change their spatial organization in the remaining membranous structure at the cell surface (*23*). Today, detergent resistance is still considered to be a useful method for characterizing the affinity for lipid rafts, but great care must be taken in using this methodology, as it may be prone to artifacts (*25*). First, not all of the proteins recovered in DRMs are in rafts and vice versa. Furthermore, recent studies on model membranes have shown that detergents (used at low temperatures) might bring membranes to a different thermodynamic state, thereby inducing a substantial reorganization of the membrane components (*26*, *27*).

Model membrane studies carried out on ternary mixtures of cholesterol, glycerophospholipids, and sphingolipids show that l_o phases, enriched in sphingolipids, separate from l_d phases, enriched in glycerophospholipids (*20*, *24*). Although the raft issue is still much debated, several observations indicate that these "artificial rafts" are a reasonable model of rafts in cell membranes (*28*). Therefore, model bilayers provide an invaluable tool for elucidating the key mechanisms of raft assembly. Several GPI-APs have been incorporated into diverse sets of artificial membranes, and their raft partitioning behavior has been examined further with biochemical methodologies (*19*, *29*), optical imaging (*30*), and AFM (*31*) techniques. Information about dynamics in model membranes has proven to be crucial in identifying phases and their molecular composition, but the focus has mainly concerned the lipid dynamics, studied by either fluorescence recovery after photobleaching (FRAP) (*30*, *32*) or fluorescence correlation spectroscopy (FCS) (*33*, *34*). Data on protein dynamics in model rafts are still very limited (*30*).

Here, we present a detailed analysis of the raft partitioning behavior of a GPI-AP, the human placental alkaline phosphatase (PLAP), in the context of its spatial distribution and dynamic behavior in domain-forming giant unilamellar vesicles (GUVs), by applying fluorescence confocal imaging and FCS. PLAP only partially associates with the l_o phase, and the affinity for this phase is shown to increase upon antibody-mediated cross-linking. Furthermore, the action of a nonionic detergent on PLAP-containing GUVs is analyzed, and a relation between membrane microdomains and DRMs is determined.

MATERIALS AND METHODS

Chemicals. 1,2-Dioleoyl-*sn*-glycero-3-phosphocholine [dioleoylphosphatidylcholine (DOPC)], *N*-stearoyl-D-erythrosphingosylphosphorylcholine [stearoylsphingomyelin (SM)], and cholesterol were purchased from Avanti Polar Lipids. Porcine brain ganglioside GM1 (GM1) was from Calbiochem. 3,3′-Dioctadecyloxacarbocyanine perchlorate (DiO-C_{18}), 1,1′-dioctadecyl-3,3,3′,3′-tetramethylindocarbocyanine perchlorate 3,3′-dioctadecyloxacarbocyanine perchlorate (DiI-C_{18}), and the AlexaFluor 488 (AF488−CTXB) and AlexaFluor 633 (AF633−CTXB) conjugates of cholera toxin B subunit were from Molecular Probes. The detergents octyl glucoside (OG), 3-[(3-cholamidopropyl)dimethylammonio]-1-propanesulfonic acid (CHAPS), and Triton X-100 were purchased from Sigma. All other chemicals were reagent grade.

Preparation of Large Unilamellar Vesicles (LUVs). Liposomes were prepared by freezing and thawing, followed by extrusion. Briefly, lipids in chloroform/methanol (9:1, v:v) solutions were mixed, dried under nitrogen, and suspended in phosphate-buffered saline (PBS) [150 mM NaCl and 100 mM phosphate buffer (pH 7.4)] or water. The obtained multilamellar vesicles were then submitted to 10 cycles of freezing into liquid nitrogen and thawing in a water bath at 50 °C, which was followed by extrusion through 0.1 μm polycarbonate membranes. Unless indicated otherwise, LUVs were composed of only DOPC or SM, DOPC, and cholesterol (1:1:1). In some experiments, the fluorescent lipid probe DiO-C_{18} and/or the ganglioside GM1 was added in the amount of 0.1 mol % for confocal imaging and 0.001 mol % for FCS. Since GM1 is known to change the lipid spatial distribution above 2 mol % (*35*, *36*), the compound was used here in minimal amounts.

Protein Purification. PLAP was purified from partially pure human placental tissue from Sigma (catalog no. P3895), as previously described (*19*). The amount of PLAP obtained from 25 mg of partially pure PLAP was resuspended in 500 μL of 0.1 M bicarbonate buffer (pH 8.3) and labeled with 0.5 mg of NHS−rhodamine (Pierce, Rockford, IL) freshly dissolved in 50 μL of DMSO, and the solution was incubated for 2 h at 4 °C in the dark, with rocking. The solution was warmed to 37 °C for 5 min; phases were separated in a microfuge, and the aqueous phase was discarded. CHAPS (200 μL, 35%) in PBS was added, and the mixture was incubated overnight at 4 °C and then loaded onto a Sephacryl 200 column (25.5 cm × 0.35 cm) pre-equilibrated with PBS and 2% CHAPS. Additional PBS and 2% CHAPS were loaded, and 40 × 0.4 mL fractions were collected. PLAP activity was checked by using a kit from Sigma. To remove residual free rhodamine (Rh), the protein was transferred to a YM-50 spin column (Millipore, Bedford, MA), subjected to centrifugation by following the instructions of the supplier, and washed with PBS and 2% CHAPS until the flow-through was colorless. Rh-labeled PLAP was analyzed for purity and to estimate the protein concentration by comparison with known amounts of bovine serum albumin by SDS−PAGE and ammoniacal silver staining. The degree of labeling was approximately one dye molecule per PLAP monomer.

Purple membranes, isolated from *Halobacterium salinarium* according to the method of Oesterhelt and Stoeckenius (*37*), were a gift from L.-O. Essen (Max Planck Institute, Martinsried, Germany). Bacteriorhodopsin (BRh) was solubilized in a 100 mM octyl glucoside (OG) solution in 25 mM phosphate buffer (pH 6.9) at a detergent-to-protein ratio of 20 (w:w). After being sonicated for 20 s, the sample was incubated in the dark at 37 °C for 1 h and then at room temperature for 20 h. Solubilization was confirmed by the inability of BRh to sediment after centrifugation at 200000*g* for 1 h. The quality of the preparation was checked by spectrophotometry; the solubilisate did not contain aggregates, and only trace amounts of free retinal were present. BRh was then labeled with AlexaFluor 488 (Molecular Probes) in the detergent state. Conjugation was performed by reacting the succinimidyl ester moiety of the dye with the primary amines present in the protein in bicarbonate buffer at pH 8. The protein conjugate was then separated from unreacted dye by gel filtration; the degree of labeling amounted 0.8−1.0 bound dye molecules per BRh.

Protein Reconstitution into Large Unilamellar Vesicles (LUVs). PLAP was reconstituted into large unilamellar vesicles (LUVs), as previously described (*28*, *29*). Briefly,

300 μg of PLAP (PBS and 2% CHAPS), unless indicated otherwise, was added to ~3 mg of the lipid vesicle suspension (PBS, 5 mM final concentration, 100 nm vesicle diameter). Detergent was subsequently removed by extensive dialysis against PBS for 2−3 days at 4 °C for LUVs composed of DOPC, and for 1−2 days at room temperature for LUVs composed of SM, DOPC, and cholesterol (1:1:1). The protein concentration in liposomes was checked by Coomassie Blue staining of an SDS gel. PLAP association with the liposomes was assessed by floating the liposomes on a discontinuous sucrose gradient. Proteoliposomes were added to 45% sucrose in PBS. Onto this suspension was layered 35% sucrose in PBS and only PBS buffer. The gradient was centrifuged at 100000*g* for 6 h at 4 °C. Fractions were taken from the gradient and analyzed with the spectrofluorimeter. Integration of PLAP in the membrane was assayed by floating the proteoliposomes in a sucrose gradient (same as before) in the presence of salty buffer [0.1 M Na_2CO_3 (pH 11)]. The salty buffer did not dissociate the protein from the membrane.

BRh was reconstituted into LUVs, as described previously (*38*). Briefly, OG was added to preformed LUVs (100 nm in diameter) in a 10:1 detergent:lipid molar ratio (50 mM OG and 5 mM lipid). After being incubated for 10 min, BRh in the detergent state was added. The detergent/lipid/protein mixture was kept at room temperature for 15 min, after which the detergent was removed by dialysis. Bio-Beads were placed in contact with the liposomes for 1−2 h (9 mg of Bio-Beads for 1 μmol of detergent), and the rest of the detergent was removed by dialysis against the buffer for 1 day by placing Bio-Beads outside the dialysis membrane. The degree of reconstitution was determined by measuring the absorbance at 560 nm ($\epsilon_{560} = 54\,000\ M^{-1}\ cm^{-1}$). Integration of BRh in the membrane was assayed by flotation of the proteoliposomes in a sucrose gradient in the presence of salty buffer [0.1 M Na_2CO_3 (pH 11)], as described for PLAP.

Preparation of Giant Unilamellar Vesicles (GUVs). GUVs prepared solely from lipids were obtained by electroformation (*39*, *40*). With this approach, single-bilayer vesicles are produced with sizes varying from 10 to 100 μm. The flow chamber (closed-bath perfusion chamber, RC-21, Warner Instruments Co.) used for vesicle preparation has been previously described (*34*). Lipids in a 9:1 chloroform/methanol mixture (5 mM) were deposited on preheated ITO coverslips, and the solvent was evaporated at 55 °C. After water had been added to the chamber (~300 μL), a voltage of 1.1 V at 10 Hz was applied for 1 h. After lipid swelling, the chamber was put directly at room temperature or cooled slowly by using a heat block. Both cooling procedures led to the same type of vesicles and domain pattern. Also, the presence of the reducing agent dithiothreitol (DTT, final concentration of 2 mM), to prevent possible lipid oxidation, did not affect domain formation or lipid mobility under our conditions of GUV formation. GUVs were always prepared from fresh lipid mixtures and kept under a nitrogen atmosphere as much as possible. Lipids were checked for oxidation by UV−vis spectroscopy and thin-layer chromatography. Under the conditions of GUV preparation, it was found that less than 0.1% of the lipids was oxidized.

Protein Reconstitution into Giant Unilamellar Vesicles. A novel reconstitution technique was developed to insert membrane proteins into GUVs. Proteo-LUVs (5 mM lipid suspension) with a sub-micrometer diameter (typically, 100 nm) were centrifuged at 200000*g* for 1 h, and the pellet was gently resuspended in Milli-Q water containing 5−10% (v:v) ethylene glycol to a final lipid concentration of 20−50 mM. The vesicle suspension was then deposited onto ITO-coated coverslips and put in the vacuum at 4 °C overnight. During membrane dehydration at low temperatures, the vesicles underwent fusion and formed large patches of membranes. Ethylene glycol is a well-known cryoprotectant agent and was used to preserve protein activity. In some experiments, 10−30 mM trehalose was used instead of ethylene glycol without observing any difference in the quality of the final GUV preparation. Note that both PLAP and BRh are very stable and resistant proteins, and therefore, the use of cryoprotectants (type and concentration) might not be critical to the final result. When the protocol was applied to other membrane proteins, the conditions of dehydration were optimized according to each particular case (N. Kahya, unpublished results). After dehydration, liposomes were rehydrated in 10 mM phosphate buffer (pH 7.2) upon an alternate electric field in the flow chamber, as described previously for the GUV preparation. After 3−4 h, numerous unilamellar vesicles formed, with a diameter varying between 10 and 150 μm. After vesicle preparation, we also exchanged the buffer with a 50 mM phosphate buffer (pH 7.2), but no changes in the results were observed. In the case of lipid mixtures at high phase transition temperatures, membranes were first rehydrated under the electric field at 55 °C for $^1/_2$ h and then cooled for the following 2−3 h.

Activity of PLAP reconstituted into GUVs was verified by using a fluorescence assay kit for alkaline phosphatases from Sigma (Starbright Alkaline Phosphatase Detection Kit, #MT-1000). Briefly, the provided substrate is a fluorogenic substrate specific for the detection of alkaline phosphatases, which cleave the phosphate group of the nonfluorescent substrate, thereby releasing free fluorescein-like dye (absorption at 450 nm, emission around 505 nm). For BRh, activity was assayed as previously described (*41*).

Confocal Fluorescence Microscopy and Fluorescence Correlation Spectroscopy (FCS). Confocal fluorescence microscopy and FCS were performed on a commercial ConfoCor2 instrument (Zeiss, Jena, Germany). Confocal images were taken with the laser scanning microscopy (LSM) module. The excitation light of an Ar ion laser at 488 nm and of a HeNe laser at 543 nm was reflected by a dichroic mirror (HFT 488/543) and focused through a Zeiss C-Apochromat 40×, NA = 1.2 water immersion objective onto the sample. The fluorescence emission was re-collected by the same objective and split by another dichroic mirror (NFT 545) into two channels. Detection of the fluorescence emission, after passing a 505−530 nm band-pass filter in the first channel and a 560 nm long-pass filter in the second channel, was obtained with two photomultipliers (PMTs). The confocal geometry was ensured by pinholes (60 μm) in front of the PMTs. FCS measurements were performed by epi-illuminating the sample with the 543 nm HeNe laser ($I_{ex} \approx 1.2\ kW/cm^2$). The excitation light was reflected by a dichroic mirror (HTF 543) and focused onto the sample by the same objective that was used for the LSM. The fluorescence emission was re-collected back and sent to an avalanche photodiode via a 560−615 nm band-pass filter.

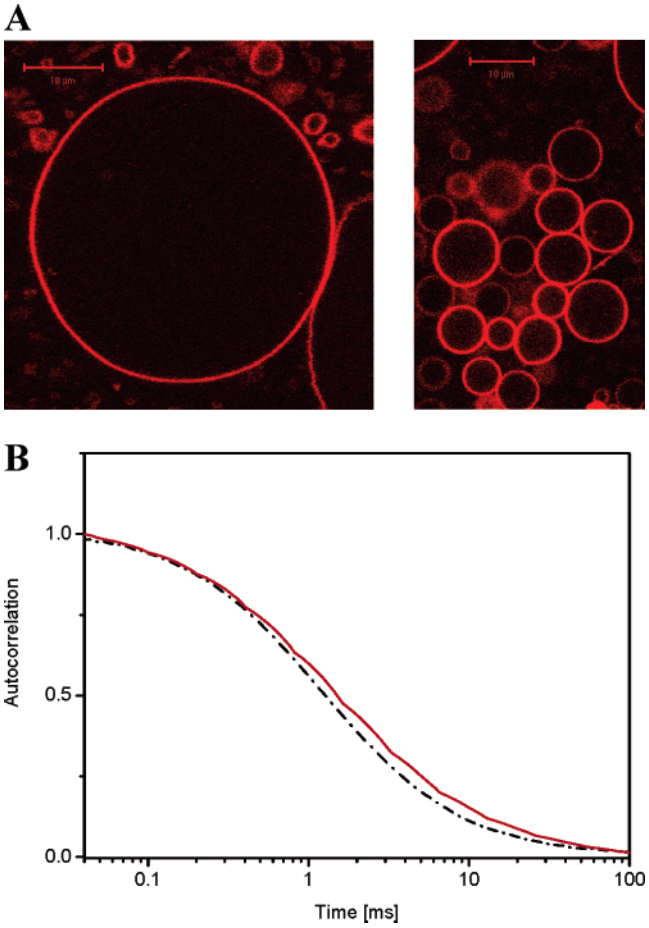

FIGURE 1: (A) Confocal image at the equator of human PLAP-containing GUVs (composed of DOPC) showing a homogeneous fluorescence from Rh-labeled PLAP corresponding to a single fluid phase. (B) The FCS curve was recorded for the PLAP-containing GUVs (composed of DOPC, solid line). The correlation trace decays more slowly than that of DiO-C_{18} in GUVs (composed of pure DOPC, dashed line), recorded in the absence of PLAP.

Out-of-plane fluorescence was reduced by a pinhole (90 μm) in front of the detector. The laser focus was positioned on the top or bottom side of GUVs, by performing an axial (z) scan through the membrane prior to the FCS recording. The fluorescence temporal signal was recorded, and the autocorrelation function $G(\tau)$ was calculated, according to the method of Magde et al. (*42*). The apparatus was calibrated by measuring the known three-dimensional diffusion coefficient of rhodamine in solution. The detection area on the focal plane was approximated to a Gaussian profile and had a radius of $\approx$0.18 μm at a relative intensity of $1/e^2$. Data fitting was performed with the Levenberg−Marquardt nonlinear least-squares fit algorithm (ORIGIN, OriginLab, Northampton, MA). The fitting equation made use of a two-dimensional Brownian diffusion model, assuming a Gaussian beam profile:

$$G(\tau) = \frac{\sum_i \langle C_i \rangle \left(\frac{1}{1 + \tau/\tau_{d,i}} \right)}{A_{eff} \left(\sum_i \langle C_i \rangle \right)^2}$$

where $\langle C_i \rangle$ is the two-dimensional time average concentration

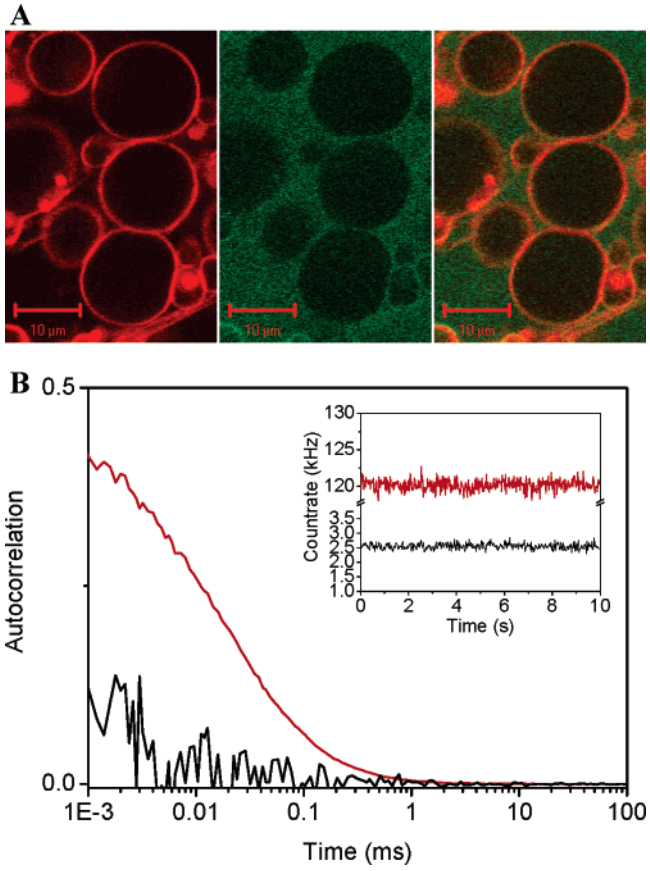

FIGURE 2: Human PLAP is functional after reconstitution into GUVs. (A) Confocal image at the equator of human PLAP-containing GUVs (DOPC) showing homogeneous fluorescence from Rh-labeled PLAP (red). The green signal, as recorded after 1.5 h, corresponds to a fluorescein-like dye produced after the enzymatic reaction (see Materials and Methods). Note the higher signal level outside the GUVs compared to that in the lumen of the vesicles. (B) The FCS curve from fluorescence of the free dye was recorded outside the PLAP-containing GUVs after $^1/_2$ h (red line). After that time, the amplitude of FCS became too low to give a reasonable signal:noise ratio, because of the high concentration of free dye produced by PLAP. The black line corresponds to the FCS curve recorded soon after addition of the substrate to the pool of GUVs. The corresponding fluorescence count rates as a function of time are reported in the inset.

of species i in the detection area A_{eff} and $\tau_{d,i}$ is the average residence time of species i. The diffusion coefficient D_I for species I is proportional to $\tau_{d,i}$. For FCS measurements, three independent GUV preparations were analyzed, and for each of them, data from at least 20 different GUVs were recorded with an acquisition time of 100 s per FCS measurement. When membrane phase separation was visualized with the LSM, the laser focus was always positioned onto one phase only for the FCS experiment.

Molecular partition coefficients in lipid phases (gel-to-l_d or l_o-to-l_d) were measured by fluorescence intensity analysis of confocal images and by measuring the number of molecules in the focal volume by FCS.

RESULTS

Human Placental Alkaline Phosphatase (PLAP) Is Effectively and Functionally Reconstituted into Giant Unilamellar Vesicles (GUVs). PLAP was reconstituted into GUVs composed of 100 mol % DOPC at an ~1:2000 protein:lipid molar ratio. GUVs were unilamellar (>85%) and presented

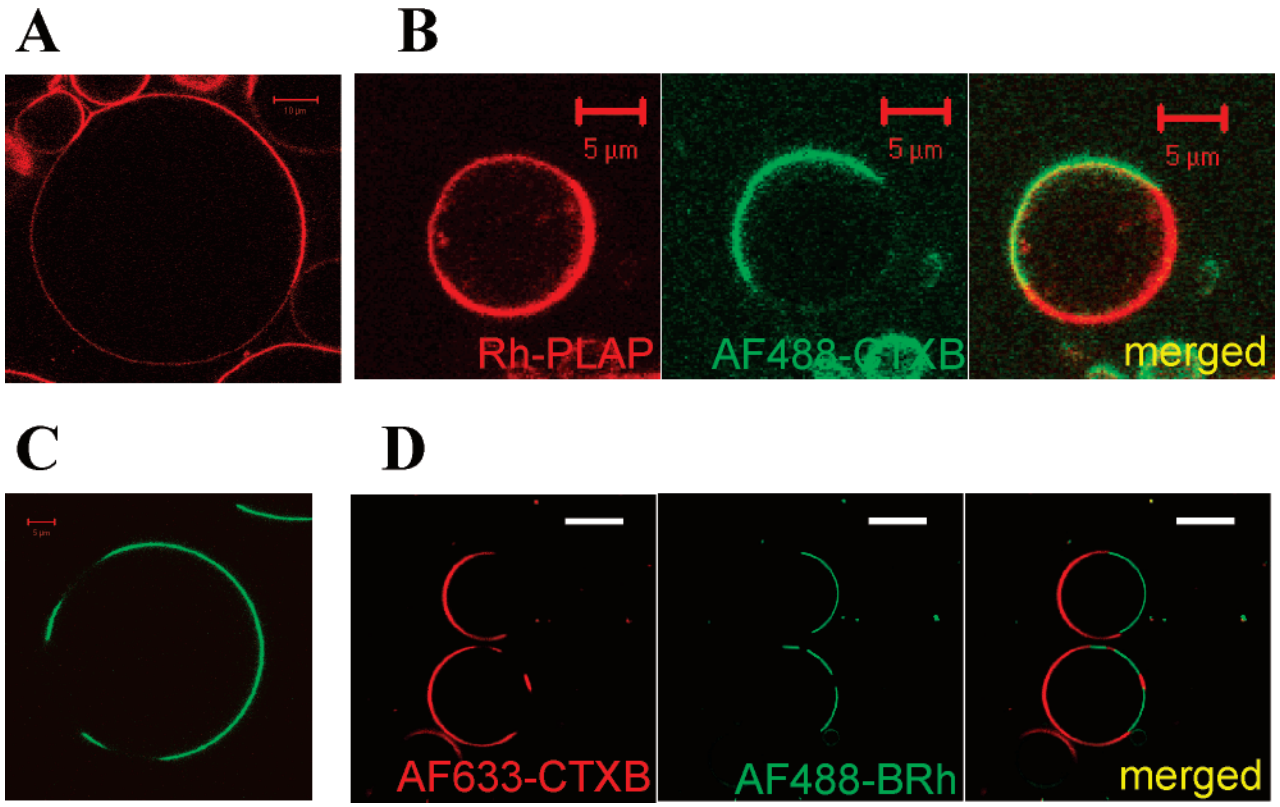

FIGURE 3: (A) Visualization of phase separation in GUVs prepared from ternary lipid mixtures of SM, DOPC, and cholesterol (1:1:1), in which human PLAP (Rh-labeled) was reconstituted (protein:lipid ratio of 1:2000). PLAP preferentially partitioned in one of the two phases with a partition coefficient of ~4. (B) Dual-color confocal image of PLAP-containing GUVs (1:1:1 SM/DOPC/cholesterol and 0.1 mol % GM1). GUVs were incubated with AF488−CTXB for 15 min. Rh-labeled PLAP (red signal, left panel) was distributed in membrane areas, which were complementary to those in which AF488−CTXB (green signal, center panel) was localized. The merged image is shown in the right panel. (C) Confocal image at the equator of a GUV (1:1:1 SM/DOPC/cholesterol), in which BRh (AF488-labeled) was reconstituted at a protein:lipid ratio of 1:1000. BRh preferentially partitions in one of the two phases with a partition coefficient of ~50. (D) Dual-color confocal image of BRh-containing GUVs (1:1:1 SM/DOPC/cholesterol and 0.1 mol % GM1). GUVs were incubated with AF633−CTXB for 15 min. AF488-labeled BRh (green signal, center panel) was distributed in membrane areas, which were complementary to those in which AF633−CTXB (red signal, left panel) was localized. The merged image is shown in the right panel.

a very regular bilayer structure (see Figure 1A). Protein lateral diffusion was assessed by FCS, yielding correlation curves (Figure 1B) which were fitted to a one-component Brownian diffusion model. The lateral diffusion coefficient of PLAP was $(5.0 \pm 0.3) \times 10^{-8}$ cm^2/s, slightly lower than that of lipids in DOPC vesicles [$D = (6.3 \pm 0.3) \times 10^{-8}$ cm^2/s], as previously measured (*34*). PLAP activity was assayed by fluorescence confocal imaging and FCS (Figure 2). The substrate, which was added after proteo-GUV formation, reacted with PLAP, resulting in the release of fluorescein-like dye in the medium, mostly outside of GUVs. Green fluorescence from dye molecules freely diffusing in the medium was readily monitored after 1.5 h by confocal imaging (see Figure 2A), and, already after $^1/_2$ h, by FCS [$D = (280 \pm 5) \times 10^{-8}$ cm^2/s; see the red line in Figure 2B; the corresponding fluorescence count rate as a function of time is shown in the inset as a red line]. As a control, soon after addition of the substrate to PLAP-containing GUVs, no signal could be detected (see the fluorescence count rate as a function of time as reported in the inset of Figure 2B, black line), and FCS curves with very low amplitudes were recorded (Figure 2B, black line). In the absence of PLAP, no fluorescence signal was detected over a 12 h time period (not shown). The results indicated that PLAP was functionally reconstituted into GUVs.

PLAP Preferentially Partitions in the l_d Phase in GUVs Composed of SM, DOPC, and Cholesterol with Some Affinity for the l_o Phase. As shown previously by our group and others (*32*, *34*−*36*), GUVs, which are composed of SM, DOPC, and cholesterol (1:1:1), form large and round domains, revealing the coexistence of fluid lipid phases. By applying FCS, we have shown that within the range of composition of phase segregation, the two phases at equilibrium exhibit diffusion coefficients which are typical of l_d and l_o phase. We reconstituted Rh-labeled PLAP into domain-forming GUVs (1:1:1 SM/DOPC/cholesterol) and imaged confocally its spatial organization in the bilayer. As shown in Figure 3A, PLAP preferentially partitioned into one lipid phase, the partition coefficient between the two phases being ~4. At the protein:lipid molar ratio used in this study (~1:2000), no change in domain morphology, bilayer structure, and/or stability was observed in the presence of PLAP in GUVs. As shown in Figure 3B, dual-color confocal imaging was performed on PLAP-containing GUVs composed of SM, DOPC, and cholesterol (1:1:1) and 0.1 mol % GM1. GM1 was used as a raft marker and could be localized upon binding of AF488−CTXB. The amount of GM1 present was kept small to prevent any change in the domain morphology and spatial distribution of the membrane components. Rh-labeled PLAP (Figure 3B, red) was shown to partition into phase regions complementary to the GM1-enriched ones (Figure 3B, green), implying a preferential partitioning of the GPI-anchored protein in the l_d phase.

As a comparison, BRh was inserted into GUVs prepared from the same lipid composition as for PLAP (1:1:1 SM/DOPC/cholesterol) at a similar protein:lipid ratio. The resulting GUVs exhibited large domains where a preferential distribution of BRh into one of the two domains could be readily detected (see Figure 3C). The partition coefficient was ~50, analogous to that measured in previous studies for the lipid probes DiI-C_{18} (*34*) and DiO-C_{18} (N. Kahya, unpublished results) in GUVs prepared from the same lipid composition. Dual-color imaging was performed to confirm BRh preferential partitioning into the l_d phase. Namely, 0.1 mol % GM1 was incorporated into GUVs composed of SM, DOPC, and cholesterol (1:1:1), and AF633−CTXB was added after vesicle formation to localize GM1 and the l_o phase. As shown in Figure 3D, AF633−CTXB (red) specifically bound to membrane regions devoid of BRh (green), implying the preferential partitioning of BRh into the l_d phase.

In the context of the above-mentioned partition coefficients, although PLAP favored DOPC-enriched areas, ~20−30% of PLAP partitioned into the SM-enriched regions, thereby showing an affinity for the l_o phase, which was higher than that of other membrane components, such as BRh and DiO-C_{18} (not shown).

To test whether PLAP partitioning behavior was concentration-dependent, we reconstituted PLAP into SM/DOPC/cholesterol GUVs at different protein:lipid molar ratios. Figure 4A shows confocal images of PLAP-containing GUVs at 1:400 (left panel) and 1:5000 (right panel) protein-to-lipid molar ratios. The partition coefficient did not change as a function of protein density (~4).

PLAP lateral diffusion properties in GUVs composed of SM, DOPC, and cholesterol (1:1:1) were investigated by FCS. Given the size of the domains, the laser focus could be positioned on one of the two phase regions and an estimate of the diffusion coefficient allowed for an independent assignment of the phases. The FCS curves are shown in Figure 4B and report on PLAP diffusion in both the l_d phase (△) and the l_o phase (○). The fitting (solid lines) was obtained with a one-component Brownian diffusion model, giving diffusion coefficients of $(3.8 \pm 0.3) \times 10^{-8}$ cm^2/s for the PLAP-enriched, l_d phase and $(0.7 \pm 0.3) \times 10^{-8}$ cm^2/s for the l_o phase. No change in PLAP dynamics could be detected in the presence of 0.1 mol % GM1. The activity assay was positive for PLAP reconstituted into GUVs composed of SM, DOPC, and cholesterol (1:1:1) with or without 0.1 mol % GM1.

Confocal Imaging of Detergent Resistance Membranes (DRMs): Effect of Triton X-100 on PLAP-Containing GUVs (1:1:1 SM/DOPC/Cholesterol) as a Function of Temperature. PLAP has been extensively reported as a membrane protein with high affinity for rafts. These conclusions were mainly drawn from studies of detergent treatment of cell lysates and model membranes, showing that PLAP was efficiently recovered in DRMs. To investigate the relationship between PLAP-containing GUVs and DRMs, we added Triton X-100 to the GUV suspension and monitored over time the detergent effect on the membrane bilayer. In Figure 5A, time-lapse confocal images are reported showing the effect of Triton X-100 (1%, v:v) on PLAP-containing GUVs (1:1:1 SM/DOPC/cholesterol) at room temperature. First, the detergent induced extensive vesicle fission, mostly leading

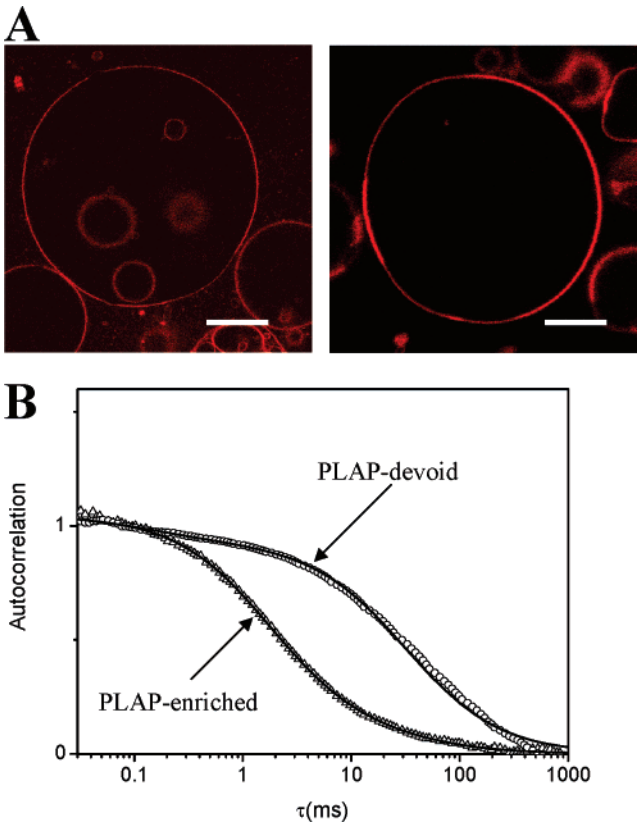

FIGURE 4: (A) PLAP preferential partitioning into the liquid-disordered phase does not depend on protein density. The figure shows confocal images of PLAP-containing GUVs (1:1:1 SM/DOPC/cholesterol) at different PLAP concentrations. PLAP was reconstituted at 1:4000 (left) and 1:500 (right) protein:lipid ratios. The bar is 10 μm. (B) Lateral diffusion of PLAP in GUVs composed of SM, DOPC, and cholesterol (1:1:1). FCS autocorrelation curves are shown for PLAP mobility in PLAP-enriched areas of GUVs (△) and PLAP-devoid areas of GUVs (○). Fitting curves (solid lines) were obtained with a two-dimensional Brownian diffusion model.

to the formation of homogeneous vesicles of distinct composition (either PLAP-enriched or PLAP-devoid; see arrows in Figure 5A). This step was followed by (sometimes it occurred simultaneously with) the solubilization of PLAP-enriched domains, whereas the PLAP-devoid vesicles resisted detergent solubilization. After the GUVs had been incubated in the chamber for 3 h, high levels of fluorescence signal were detected in the medium, indicating that PLAP was mostly solubilized (shown in Figure 5B). Some vesicles, almost completely devoid of PLAP, resisted detergent extraction and appeared as black holes against the fluorescent background. Upon addition of 10% (v:v) Triton X-100, the amount of PLAP-devoid vesicles present in the final stage decreased but the qualitative result did not change: PLAP was mostly solubilized by Triton X-100 at room temperature. Similarly, detergent extraction was also performed at 4 °C. Prior to addition of the detergent, phase separation was readily visible under the confocal microscope at 4 °C (see Figure 5C). The same domain pattern was observed in control experiments with 1:1:1 SM/DOPC/cholesterol GUVs and the lipid probe DiI-C_{18} in the absence of the protein (not shown). Interestingly, in contrast to the scenario at room temperature, when detergent treatment was performed at 4 °C, GUVs shrunk down to a smaller size but solubilization of PLAP occurred to a much less extent than at higher temperatures,

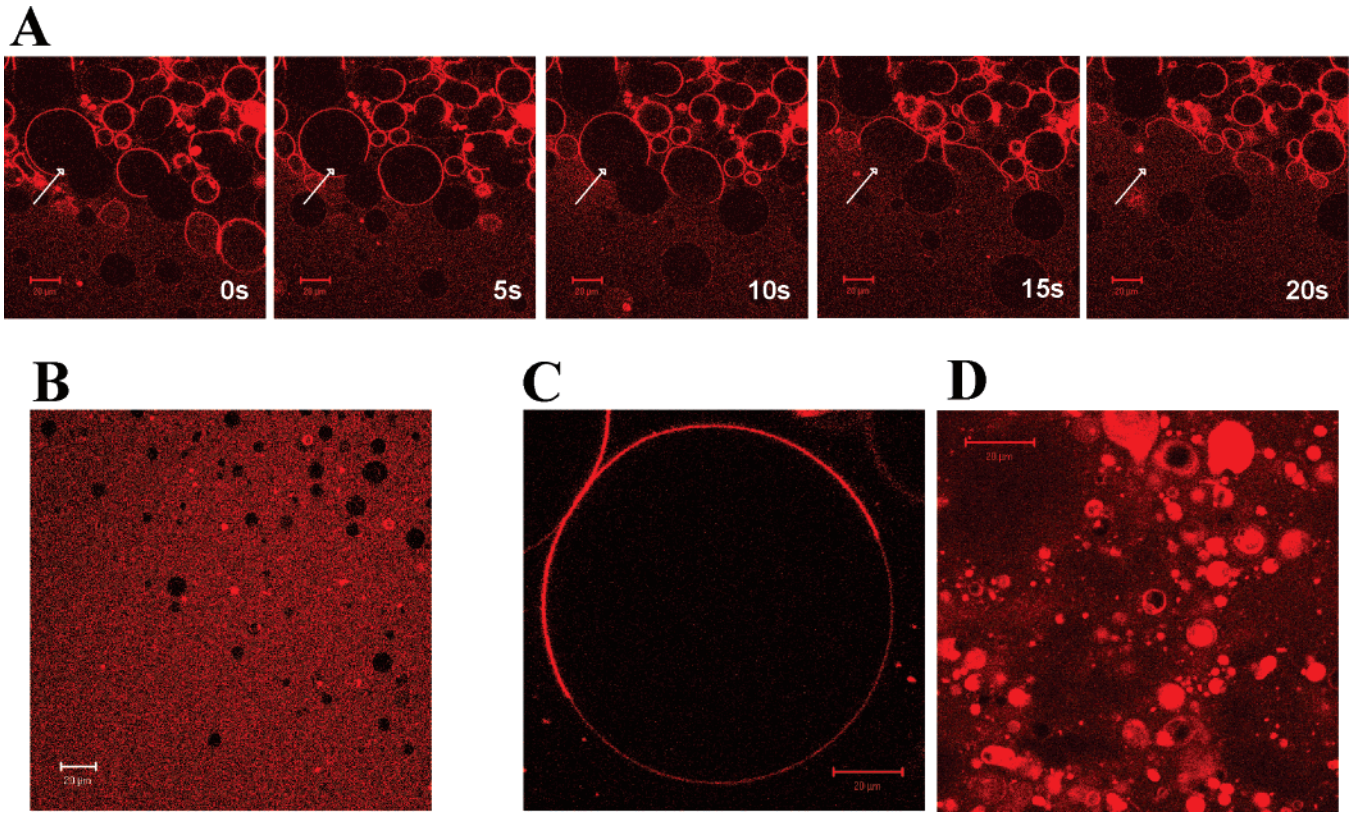

FIGURE 5: Effect of Triton X-100 extraction as a function of temperature on the distribution of human PLAP on GUVs composed of SM, DOPC, and cholesterol (1:1:1). (A) Time-lapse confocal imaging of PLAP-containing GUVs upon extraction of Triton X-100 (1%) at room temperature. (B) Confocal image of the GUV sample after incubation with Triton X-100 (1%) for 3 h at room temperature. The high background arose from the solubilized PLAP (Rh-labeled). The black holes were small PLAP-devoid vesicles resistant to the detergent. (C and D) Confocal image of PLAP-containing GUVs upon extraction with Triton X-100 (1%) at 4 °C after incubation for 10 min (C) and 3 h (D).

as the fluorescence background did not increase with time. After incubation for 3 h, the resistant membranes were reduced to vesicular structures and patches (so-called DRMs), which retained most of the fluorescence signal, whereas almost no fluorescence in the background was detected (Figure 5D). Upon addition of 10% (v:v) Triton X-100, no further solubilization of the membrane patches was observed. These results imply that PLAP resists detergent solubilization on ice, thereby allowing for efficient recovery of the protein in the DRMs. PLAP was found to be active at 4 °C, although the kinetics of cleavage of the phosphate group of the substrate was ~10-fold lower than at room temperature.

To rule out the possibility that the GUV preparation was affected by artifacts, we carried out detergent extraction of PLAP in LUVs with a 1:1:1 SM/DOPC/cholesterol composition. As for the experiments with GUVs, PLAP was recovered in the DRMs upon addition of 1−10% (v:v) Triton X-100 on ice but was almost completely solubilized upon addition of 10% (v:v) Triton X-100 at room temperature. LUVs, which were submitted to incubation for 3 h at 55 °C, yielded the same results as those that did not undergo preheating, implying that the preheating step for GUV preparation did not affect PLAP activity and detergent resistance.

BRh reconstituted into GUVs composed of SM, DOPC, and cholesterol (1:1:1) was also tested for detergent resistance: solubilization of most of the protein was readily monitored at both room temperature and 4 °C. As shown in Figure 6A, detergent solubilization of BRh was monitored on-line at room temperature, leading to a very high background signal after incubation for 3 h with 1−10% Triton X-100 (Figure 6B). Detergent extraction was repeated at 4 °C. Prior to detergent treatment, vesicles exhibited the same domain pattern as at room temperature (see Figure 6C). Upon addition of detergent, BRh was almost completely solubilized by Triton X-100 (1−10%), in a manner very similar to the treatment at room temperature (see Figure 6D).

Antibody-Mediated Cross-Linking of PLAP Induces a Higher Affinity for the l_o Phase. We wanted to investigate whether PLAP changed partitioning behavior between the l_d and l_o phase upon cross-linking. The most usual way to induce cross-linking, although it might not be the most physiological one, is by binding of an antibody. Therefore, after reconstitution into GUVs (1:1:1 SM/DOPC/cholesterol), PLAP was cross-linked by using a polyclonal antibody against PLAP from rabbit. The GUVs were incubated for $^1/_2$−3 h at 37 °C and then imaged confocally. PLAP cross-linking induced a change in the domain morphology, as shown in Figure 7, where PLAP distribution in GUVs before (Figure 7A) and after (Figure 7B) antibody binding are compared. The partition coefficient of the protein also shifted from 4:1 before cross-linking (Figure 7A) to 2:1 up to 1.5:1 after antibody binding (Figure 7B). This is evident from the intensity profiles measured across the equatorial slices of GUVs before (Figure 7C) and after (Figure 7D) cross-linking. Furthermore, in 30% of the vesicles, PLAP-containing GUVs

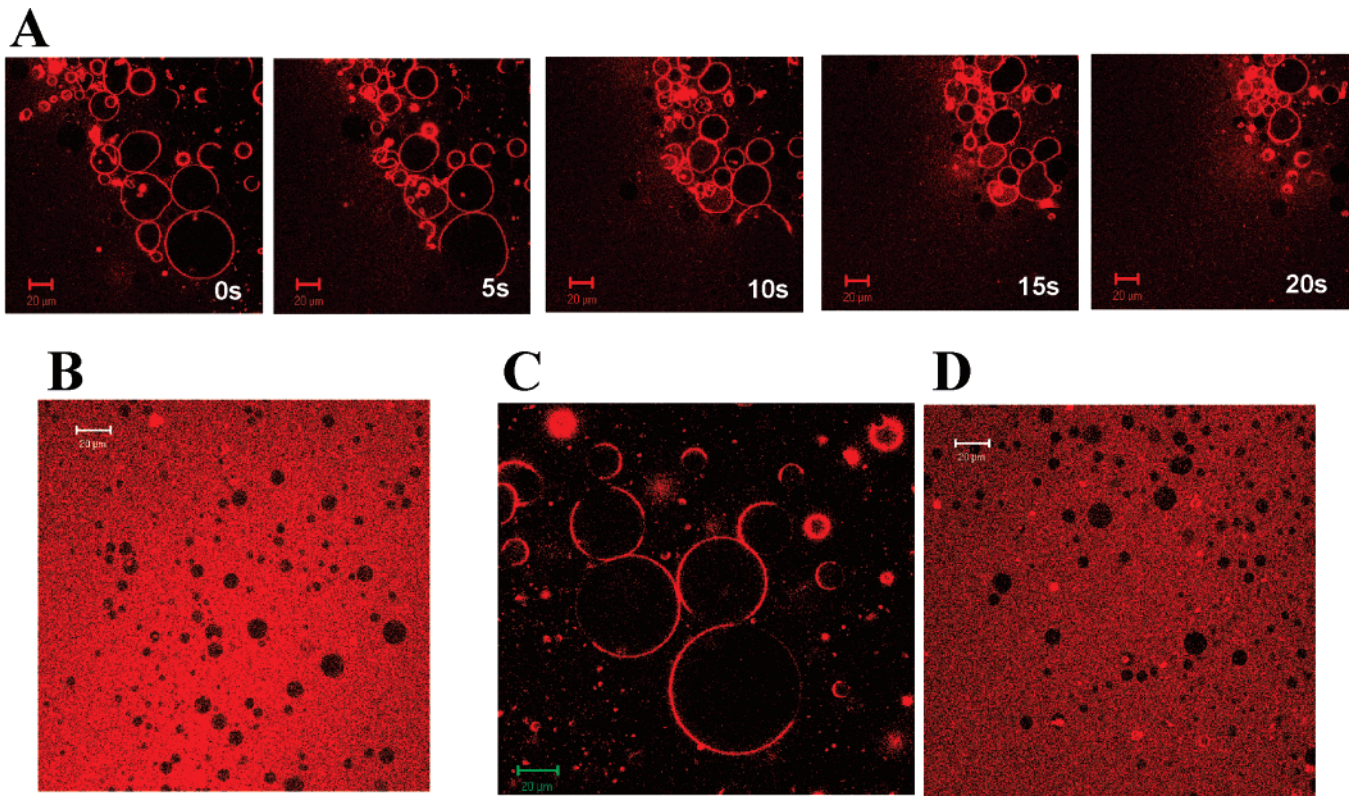

FIGURE 6: Effect of Triton X-100 extraction as a function of temperature on the distribution of BRh on GUVs composed of SM, DOPC, and cholesterol (1:1:1). (A) Time-lapse confocal imaging of BRh-containing GUVs upon extraction of Triton X-100 (1%) at room temperature. (B and C) Confocal images of the GUV sample after incubation with Triton X-100 (1%) for 3 h at room temperature (B) and 4 °C (C). The high background arose from the solubilized BRh (AF488-labeled). The black holes were small BRh-devoid vesicles resistant to the detergent.

did not exhibit raftlike domains after cross-linking and fluorescence from PLAP was uniformly distributed on the GUV surface. We also repeated the experiment in the presence of 0.1% GM1 to localize SM-enriched areas. Those PLAP-containing vesicles that did not exhibit phase separation efficiently bound AF488−CTXB (see Figure 7E), leading to a complete overlap of the PLAP signal (red, Figure 7E) with that from AF488−CTXB (green, Figure 7E).

DISCUSSION

Lipid raft assembly has been previously visualized by optical microscopy in several model membranes, including monolayers (*30*, *43*), supported planar bilayers (*30*, *44*), and free-standing giant vesicles (*32*, *34*, *45*, *46*). So far, reconstitution of membrane proteins in heterogeneous membranes was carried out in monolayers (*32*) and supported planar bilayers (*31*, *43*), whereas the spatial organization of membrane proteins in domain-forming giant unilamellar vesicles (GUVs) was never investigated. Here, we developed a tool that allows for investigation of the raft morphology in GUVs in the presence of putative raft-targeted membrane proteins. Key parameters such as partition coefficients for lipid phases and lateral diffusion coefficients were determined for the human PLAP, as reconstituted into domain-forming GUVs. Less than 30% of the PLAP population showed affinity for the l_o phase, whereas the extent of raft association increased upon antibody-mediated cross-linking. The distribution of PLAP in distinct phases of the GUVs membranes was compared to that of a nonraft protein, BRh. We also attempted to identify a relation between domain-forming giant vesicles and DRMs, by monitoring the fate of PLAP in both systems.

GPI-anchored proteins represent a large class of functionally diverse proteins, whose common feature is their association to the membrane via a post-translational modification, the GPI anchor (*2*, *3*). A large fraction of GPI-APs has been found in the exoplasmic leaflet of the plasma membrane in eukaryotes (*2*, *47*), although GPI-APs have also been localized in other membrane compartments, i.e., in the ER, the Golgi, and exo- and endocytic vesicles (*3*). The function of several GPI-APs has been shown to depend on sphingolipid and cholesterol levels in live cells. Importantly, experimental evidence from Brown and Rose demonstrated that GPI-APs, including PLAP, are recovered in DRMs isolated from cell lysates (*11*). Later on, extensive studies have identified a clear correlation between the insolubility of PLAP and other GPI-APs in vivo and that in model membranes (i.e., LUVs) (*27*, *28*). In both cases, the protein insolubility behavior depends on sphingolipid and cholesterol levels. These results have consequently led to the idea that a good correlation exists between detergent insolubility of GPI-APs and their presence in the lipid l_o phase, and hence in rafts. However, in early studies (*21*), it was emphasized that the requirement of insolubility in the presence of nonionic detergents might be necessary but not sufficient in probing raft targeting of membrane components. In the case of GPI-APs, early work by Mayor and Maxfield (*21*) showed significant protein reorganization at the cell surface after detergent extraction. Those results led to the conclusion that native rafts in resting cells might contain only a relatively

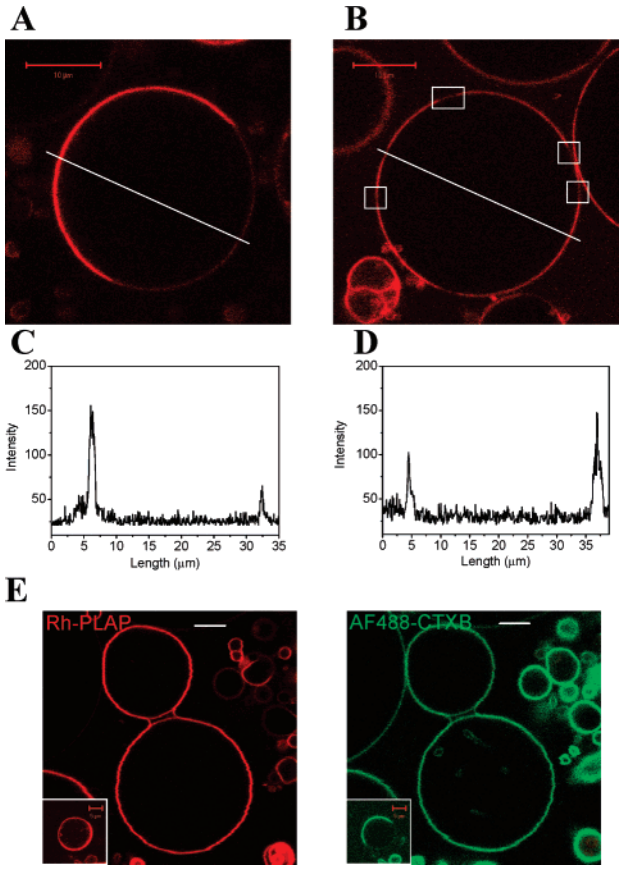

FIGURE 7: Antibody-mediated cross-linking of human PLAP induces a redistribution on the vesicle surface between the SM-enriched and DOPC-enriched phase. (A and B) Confocal image of human PLAP reconstituted into GUVs composed of SM, DOPC, and cholesterol (1:1:1) before (A) and after (B) cross-linking with a polyclonal antibody against human PLAP (for details, see Materials and Methods). PLAP-devoid domains (in the squares in panels B) after antibody binding appear to be more fragmented. Also, PLAP exhibited an increased affinity for the SM-enriched phase, as the partitioning coefficient between the l_d and l_o phases shifted from ~4 before to ~1.5 after cross-linking. (C and D) Fluorescence intensity profiles collected from a cut line across confocal images of equatorial slices of GUVs (see the cut lines in panels A and B) before (C) and after (D) cross-linking. (E) Dual-color confocal imaging of PLAP reconstituted into GUVs (1:1:1 SM/DOPC/cholesterol) containing 0.1 mol % GM1. After incubation with AF488−CTXB, in 30% of the vesicle population Rh-labeled PLAP (red signal, left panel) accumulated in regions coincident with those in AF488−CTXB localized (green signal, right panel). The bar is 10 μm. Insets show confocal images of PLAP-containing GUVs (1:1:1 SM/DOPC/cholesterol and 0.1 mol % GM1) before cross-linking (PLAP is reported as a red signal in the left panel and AF488−CTXB as a green signal in the right panel).

low concentration of GPI-APs with respect to the rest of the membrane bilayer. Consistent with this idea, our data show that only a fraction (~20−30%) of PLAP associates with the l_o phase in GUVs composed of SM, DOPC, and cholesterol (1:1:1). A similar sorting behavior has been found for the bovine intestine alkaline phosphatase, a GPI-AP homologous to PLAP, as reconstituted in GUVs prepared from analogous lipid mixtures (N. Kahya and S. Morandat, unpublished results). Although low, the affinity for the l_o phase was found to be much higher than that of BRh in GUVs from the same lipid mixture. Furthermore, our results are also in line with a previous analysis of raft association behavior of another GPI-AP, Thy-1 (*30*). Here, at most 40% of Thy-1 was shown to partition into the l_o phase of monolayers prepared from synthetic lipid mixtures similar to those used in this study. The partitioning behavior of Thy-1 shifted in favor of the l_o phase only with more natural lipid milieu, such as in brush border membranes. These findings support the idea that the molecular packing of the l_o phase in synthetic lipid mixtures is most likely very tight and is therefore capable of including only a few foreign molecules, such as GPI-APs.

How do we reconcile these results with earlier findings obtained from DRMs? It is now widely accepted that copurification with DRM fragments alone does not provide proof of an association with pre-existing domains in cells and/or model membranes. Possible artifacts intrinsic to this technique arise from the potential coalescence of detergent insoluble components and/or removal of components caused by the action of the detergent at low temperatures. Recent studies by Heerklotz et al. (*26*, *27*) have described the potential changes occurring in the thermodynamics of the membrane system as a function of addition of detergents and change in temperature. Consistent with those findings, our data show that there is a significant difference in terms of composition and raft association of proteins and lipids between a free-standing bilayer and the DRMs, in particular, those obtained at low temperatures. In this work, only 20−30% of PLAP is targeted to the l_o phase, whereas it is mostly retained in the membrane fragments (sphingomyelin and cholesterol-enriched) after detergent extraction is carried out at 4 °C. It is reasonable to believe that functional rafts are formed on the basis of a delicate balance of lipid−lipid and lipid−protein interactions, which might be very sensitive to subtle changes in parameters, such as temperature, pressure, and (detergent-induced) changes in the molecular packing.

Recently, PLAP has also been inserted into supported planar bilayers and its spatial organization observed by AFM (*31*). Here, the protein was exclusively localized into the l_o phase of supported bilayers from synthetic lipid mixtures of SM and DOPC, both in the presence and in the absence of cholesterol. The difference in the efficiency of targeting to rafts between this and our study might be related to the use of a planar supported bilayer (with a mica surface interfaced with the lipid bilayer) and/or to its protocol of preparation. Indeed, the presence of tightly packed lipid regions (e.g., l_o phase) might prevent full and extensive fusion of PLAP-containing multilamellar liposomes, thereby impairing the formation of a regular bilayer structure. Besides, the interaction of the bilayer with the mica support could alter the lipid−lipid and lipid−protein interaction energies and, hence, induce a redistribution of the membrane components.

We have investigated the lateral diffusion properties of PLAP in distinct domains by applying FCS. According to the Saffman−Delbrück theory (*48*), a monomeric GPI-AP should ideally diffuse in the plane of the membrane at approximately the same speed of a lipid molecule. Indeed, the only part that critically determines the lateral diffusion coefficient is the GPI anchor, which spans only one membrane leaflet, as in lipids. In our study, PLAP diffuses in both l_d and l_o phases with a diffusion coefficient which is lower by a factor of ~1.4 than that of lipids in the corresponding domains, as measured in our previous study (*34*). The slow dynamics of the protein might support the idea of a nanoscale organization of GPI-APs that organize

in dense clusters, for which experimental evidence has recently been reported for live cells (*49*, *50*). However, clustering of a few subunits (two to three) cannot explain the low mobility of PLAP with respect to lipids. The protein dynamics might also reflect a rather large hydrodynamic radius of PLAP due to specific lipid or cholesterol molecules, which form a thick shell around and move together with the protein. In the most likely scenario, a combination of the two possibilities is envisioned, consistent with the report by Sharma et al. (*50*) in which the small dense protein clusters have been shown to be specifically dependent on the presence of cholesterol.

Although the issue of identifying the nature of rafts is still strongly debated (*23*, *51*, *52*), it is widely accepted that, in specific cellular contexts of sorting and signaling, larger and more stable platforms are formed. A very common way to mimic signaling is achieved by antibody-mediated cross-linking. Lateral cross-linking has been shown to induce patching of membrane proteins and lipids, leading to formation of stabilized domains (*19*). Clustering of membrane components that exhibit affinity for a certain phase region might induce cooperative effects, which strengthen the association with that phase. It has been shown in supported monolayers that chemical cross-linking of lipids shifts their partition coefficient in favor of the l_o phase with respect to the l_d phase (*30*). Consistent with those studies, we observed a smoothing of the domains and a change in the raft partitioning behavior of PLAP. This might be interpreted as a migration of the cross-linked PLAP to the l_o phase, whatever the lipid phase composition might be after clustering of the protein. Seeing the striking lateral distribution of GM1-bound AF488−CTXB after cross-linking of PLAP (in 30% of the GUVs, the signal from AF488−CTXB overlaps with that from PLAP; see Figure 7E), we face now the question of "who's organizing whom". Are the lipids moving cross-linked PLAP from one lipid phase to the other, or is the cross-linked protein that organizes lipids differently inducing a new molecular ordering of the observed domains?

In conclusion, the spatial organization of a GPI-AP, the human PLAP, in free-standing giant unilamellar vesicles has been investigated. The affinity of PLAP for raftlike domains has been shown to be strongly dependent on subtle changes in lipid−lipid and lipid−protein interaction energies, as in the case of detergent solubilization and antibody-mediated cross-linking. The challenge is now to increase the complexity of this minimal model system, closely mimic the cellular context, and explore the structural and functional architecture of lipid and protein organization in membranes.

ACKNOWLEDGMENT

Kai Simons and Dick Hoekstra are kindly acknowledged for critical reading of the manuscript and stimulating discussions. The authors are also grateful to Lucie Kalvodova for useful discussions and for providing the polyclonal antibody against PLAP and to Sandrine Morandat and Dennis Merkle for helpful feedback in the biochemistry work.

REFERENCES

1. Undenfriend, S., and Kodukula, K. (1995) How glycosyl-phosphatidylinositol-anchored membrane proteins are made, *Annu. Rev. Biochem. 64*, 563−591.
2. Ferguson, M. A. (1999) The structure, biosynthesis and functions of glycosylphosphatidylinositol anchors, and the contributions of trypanosome research, *J. Cell Sci. 112*, 2799−2809.
3. Chatterjee, S., and Mayor, S. (2001) The GPI-anchor and protein sorting, *Cell. Mol. Life Sci. 58*, 1969−1987.
4. Lublin, D. M., and Coyne, K. E. (1991) Phospholipid anchor and transmembrane versions of either decay-accelerating factor or membrane cofactor protein show equal efficiency in protection from complement-mediated cell damage, *J. Exp. Med. 174*, 35−44.
5. Itzhaky, D., Raz, N., and Hollander, N. (1998) The glycosylphosphatidylinositol-anchored form and the transmembrane form of CD58 associate with protein kinases, *J. Immunol. 160*, 4361−4366.
6. Ritter, T. E., Fajardo, O., Matsue, H., Anderson, R. G., and Lacey, S. W. (1995) Folate receptors targeted to clathrin-coated pits cannot regulate vitamin uptake, *Proc. Natl. Acad. Sci. U.S.A. 92*, 3824−3828.
7. Brown, D. (1993) The tyrosine kinase connection: How GPI-anchored proteins activate T cells, *Curr. Opin. Immunol. 5*, 349−354.
8. Ilangumaran, S., Robinson, P. J., and Hoessli, D. C. (1999) in *GPI-anchored membrane proteins and carbohydrates* (Hoessli, D. C., and Ilangumaran, S., Eds.) pp 43−69, Landes, Austin, TX.
9. Lisanti, M. P., and Rodriguez-Boulan, E. (1990) Glycophospholipid membrane anchoring provides clues to the mechanism of protein sorting in polarized epithelial cells, *Trends Biochem. Sci. 15*, 113−118.
10. Simons, K., and Wandinger-Ness, A. (1990) Polarized sorting in epithelia, *Cell 62*, 207−210.
11. Brown, D. A., and Rose, J. K. (1992) Sorting of GPI-anchored proteins to glycolipid-enriched membrane subdomains during transport to the apical cell surface, *Cell 68*, 533−544.
12. Low, M. G. (1989) The glycosyl-phosphatidylinositol anchor of membrane proteins, *Biochim. Biophys. Acta 988*, 427−454.
13. Wright, J. W., and Copenhaver, P. F. (2000) Different isoforms of Fasciclin II play distinct roles in the guidance of neuronal migration during insect embryogenesis, *Dev. Biol. 225*, 59−78.
14. Simons, K., and van Meer, G. (1988) Lipid sorting in epithelial cells, *Biochemistry 27*, 6197−6202.
15. Simons, K., and Ikonen, E. (1997) Functional rafts in cell membranes, *Nature 387*, 569−572.
16. Simons, K., and Toomre, D. (2000) Lipid rafts and signal transduction, *Nat. Rev. Mol. Cell Biol. 1*, 31−39.
17. Mayor, S., Sabharanjak, S., and Maxfield, F. R. (1998) Cholesterol-dependent retention of GPI-anchored proteins in endosomes, *EMBO J. 17*, 4626−4638.
18. Chatterjee, S., Smith, E. R., Hanada, K., Stevens, V. L., and Mayor, S. (2001) GPI anchoring leads to sphingolipid-dependent retention of endocytosed proteins in the recycling endosomal compartment, *EMBO J. 20*, 1583−1592.
19. Schroeder, R. J., London, E., and Brown, D. A. (1994) Interactions between saturated acyl chains confer detergent resistance on lipids and glycosylphosphatidylinositol (GPI)-anchored proteins: GPI-anchored proteins in liposomes and cells show similar behavior, *Proc. Natl. Acad. Sci. U.S.A. 91*, 12130−12134.
20. Brown, D. A., and London, E. (1998) Structure and origin of lipid domains in biological membranes, *J. Membr. Biol. 164*, 103−114.
21. Harder, T., Scheiffele, P., Verkade, P., and Simons, K. (1998) Lipid domain structure of the plasma membrane revealed by patching of membrane components, *J. Cell Biol. 141*, 929−942.
22. Hanada, K., Nishijima, M., Akamatsu, Y., and Pagano, R. E. (1995) Both sphingolipids and cholesterol participate in the detergent insolubility of alkaline phosphatase, a glycosylphosphatidylinositol-anchored protein, in mammalian membranes, *J. Biol. Chem. 270*, 6254−6260.
23. Mayor, S., and Maxfield, F. R. (1995) Insolubility and distribution of GPI-anchored proteins at the cell surface after detergent treatment, *Mol. Biol. Cell 6*, 929−944.
24. Brown, D. A., and London, E. (2000) Structure and function of sphingolipid- and cholesterol-rich membrane rafts, *J. Biol. Chem. 275*, 17221−17224.
25. Simons, K., and Vaz, L. C. (2004) Model systems, lipid rafts, and cell membranes, *Annu. Rev. Biophys. Biomol. Struct. 33*, 269−295.
26. Heerklotz, H. (2002) Triton promotes domain formation in lipid raft mixtures, *Biophys. J. 83*, 2693−2701.

27. Heerklotz, H., Szadkowska, H., Anderson, T., and Seelig, J. (2003) The sensitivity of lipid domains to small perturbations demonstrated by the effect of Triton, *J. Mol. Biol. 329*, 793−799.
28. Brown, D. A. (2001) Seeing is believing: Visualization of rafts in model membranes, *Proc. Natl. Acad. Sci. U.S.A. 98*, 10517−10518.
29. Schroeder, R. J., Ahmed, S. N., Zhu, Y., London, E., and Brown, D. A. (1998) Cholesterol and sphingolipids enhance the Triton X-100 insolubility of glycosylphosphatidylinositol-anchored proteins by promoting the formation of detergent-insoluble ordered membrane domains, *J. Biol. Chem. 279*, 1150−1157.
30. Dietrich, C., Volovyk, Z. N., Levi, M., Thompson, N. L., and Jacobson, K. (2001) Partitioning of Thy-1, GM1, and cross-linked phospholipid analogs into lipid rafts reconstituted in supported model membrane monolayers, *Proc. Natl. Acad. Sci. U.S.A. 98*, 10642−10647.
31. Saslowsky, D. E., Lawrence, J., Ren, X., Brown, D. A., Henderson, R. M., and Edwardson, J. M. (2002) Placental alkaline phosphatase is efficiently targeted to rafts in supported lipid bilayers, *J. Biol. Chem. 277*, 26966−26970.
32. Dietrich, C., Bagatolli, L. A., Volovyk, Z. N., Thompson, N. L., Levi, M., Jacobson, K., and Gratton, E. (2001) Lipid rafts reconstituted in model membranes, *Biophys. J. 80*, 1417−1428.
33. Korlach, J., Schwille, P., Webb, W. W., and Feigenson, G. (1999) Characterization of lipid bilayer phases by confocal microscopy and fluorescence correlation spectroscopy, *Proc. Natl. Acad. Sci. U.S.A. 96*, 8461−8466.
34. Kahya, N., Scherfeld, D., Bacia, K., Poolman, B., and Schwille, P. (2003) Probing lipid mobility of raft-exhibiting model membranes by fluorescence correlation spectroscopy, *J. Biol. Chem. 278*, 28109−28115.
35. Yuan, C., and Johnston, L. J. (2000) Distribution of ganglioside GM1 in L-α-dipalmitoylphosphatidylcholine/cholesterol monolayers: A model for lipid rafts, *Biophys. J. 79*, 2768−2782.
36. Yuan, C., Furlong, J., Burgos, P., and Johnston, L. J. (2002) The size of lipid rafts: An atomic force microscopy study of ganglioside GM1 domains in sphingomyelin/DOPC/cholesterol membranes, *Biophys. J. 82*, 2526−2535.
37. Oesterhelt, D., and Stoeckenius, W. (1974) Isolation of the cell membrane of *Halobacterium halobium* and its fractionation into red and purple membrane, *Methods Enzymol. 31*, 667−678.
38. Rigaud, J. L., Paternostre, M. T., and Bluzat, A. (1988) Mechanisms of membrane protein insertion into liposomes during reconstitution procedures involving the use of detergents. 2. Incorporation of the light-driven proton pump bacteriorhodopsin, *Biochemistry 27*, 2677−2688.
39. Angelova, M. I., and Dimitrov, D. S. (1986) Liposome electroformation, *Faraday Discuss. Chem. Soc. 81*, 303−308.
40. Dimitrov, D. S., and Angelova, M. I. (1988) Lipid swelling and liposome formation mediated by electric fields, *Bioelectrochem. Bioenerg. 19*, 323−333.
41. Kahya, N., Wiersma, D. A., Poolman, B., and Hoekstra, D. (2002) Spatial organization of bacteriorhodopsin in model membranes. Light-induced mobility changes, *J. Biol. Chem. 277*, 39304−39311.
42. Magde, D., Elson, E., and Webb, W. W. (1972) Thermodynamic Fluctuations in a Reacting System: Measurement by Fluorescence Correlation Spectroscopy, *Phys. Rev. Lett. 29*, 705−708.
43. Khan, T. K., Yang, B., Thompson, N. L., Maekawa, S., Epand, R. M., and Jacobson, K. (2003) Binding of NAP-22, a calmodulin-binding neuronal protein, to raft-like domains in model membranes, *Biochemistry 42*, 4780−4786.
44. Samsonov, A. V., Mihalyov, I., and Cohen, F. C. (2001) Characterization of cholesterol-sphingomyelin domains and their dynamics in bilayer membranes, *Biophys. J. 81*, 1486−1500.
45. Bagatolli, L. A., and Gratton, E. (2000) Two-photon fluorescence microscopy of coexisting lipid domains in giant unilamellar vesicles of binary phospholipid mixtures, *Biophys. J. 78*, 290−305.
46. Kahya, N., Scherfeld, D., Bacia, K., and Schwille, P. (2004) Lipid domain formation and dynamics in giant unilamellar vesicles explored by fluorescence correlation spectroscopy, *J. Struct. Biol. 147*, 77−89.
47. Low, M. (1999) in *GPI-anchored membrane proteins and carbohydrates*, (Hoessli, D. C., and Ilangumaran, S., Eds.) pp 1−14, Landes, Austin, TX.
48. Saffmann, P. G., and Delbrück, M. (1975) Brownian motion in biological membranes, *Proc. Natl. Acad. Sci. U.S.A. 72*, 3111−3113.
49. Varma, R., and Mayor, S. (1998) GPI-anchored proteins are organized in submicron domains at the cell surface, *Nature 394*, 798−801.
50. Sharma, P., Varma, R., Sarasij, R. C., Gousset, I. K., Krishnamoorthy, G., Rao, M., and Mayor, S. (2004) Nanoscale organization of multiple GPI-anchored proteins in living cell membranes, *Cell 116*, 577−589.
51. Kusumi, A., Koyama-Honda, I., and Suzuki, K. (2004) Molecular dynamics and interactions for creation of stimulation-induced stabilized rafts from small unstable steady-state rafts, *Traffic 5*, 213−230.
52. Mayor, S., and Rao, M. (2004) Raft: Scale-dependent, active lipid organization at the cell surface, *Traffic 5*, 231−240.

BI047429D